Impact of the Disruption of ASN3-Encoding Asparagine Synthetase on Arabidopsis Development

Laure L. Gaufichon, Anne A. Marmagne, Tadakatsu Yoneyama, Toshiharu Hase, Gilles G. Clément, Marion Trassaert, Xiaole Xu, Maryam Shakibaei, Amina Najihi, Akira A. Suzuki

Impact of the Disruption of *ASN3*-Encoding Asparagine Synthetase on Arabidopsis Development

Laure Gaufichon [1], **Anne Marmagne** [1], **Tadakatsu Yoneyama** [2], **Toshiharu Hase** [3], **Gilles Clément** [1], **Marion Trassaert** [1], **Xiaole Xu** [1], **Maryam Shakibaei** [1], **Amina Najihi** [1] and **Akira Suzuki** [4],*

[1] Institut Jean-Pierre Bourgin, INRA, AgroParisTech, CNRS, Université Paris-Saclay, RD10, 78026 Versailles Cedex, France; lgaufichon@gmail.com (L.G.); anne.marmagne@versailles.inra.fr (A.M.); gilles.clement@versailles.inra.fr (G.C.); trassaert.marion@gmail.com (M.T.); xu.xiaole1212@gmail.com (X.X.); ms.shakibaei@gmail.com (M.S.); amina.najihi64@gmail.com (A.N.)
[2] The University of Tokyo, Department of Applied Biological Chemistry, Yayoi l-1-1, Bunkyo-ku, 113-8657 Tokyo, Japan; tadakatsu_yoneyama@opal.ocn.ne.jp
[3] Osaka University, Institute for Protein Research, Suita, Osaka 565-0871, Japan; enzyme@protein.osaka-u.ac.jp
[4] INRA, IJPB, UMR1318, ERL CNRS 3559, Saclay Plant Sciences, RD10, F-78026 Versailles, France
*   Correspondence: Akira.Suzuki@versailles.inra.fr; Tel.: +33-(0)1-30-83-32-28; Fax: +33-(0)1-30-83-30-96

Abstract: The aim of this study was to investigate the role of *ASN3*-encoded asparagine synthetase (AS, EC 6.3.5.4) during vegetative growth, seed development and germination of *Arabidopsis thaliana.* Phenotypic analysis of knockout (*asn3-1*) and knockdown (*asn3-2*) T-DNA insertion mutants for the *ASN3* gene (At5g10240) demonstrated wild-type contents of asparagine synthetase protein, chlorophyll and ammonium in green leaves at 35 days after sowing. *In situ* hybridization localized *ASN3* mRNA to phloem companion cells of vasculature. Young siliques of the *asn3-1* knockout line showed a decrease in asparagine but an increase in glutamate. The seeds of *asn3-1* and *asn3-2* displayed a wild-type nitrogen status expressed as total nitrogen content, indicating that the repression of *ASN3* expression had only a limited effect on mature seeds. An analysis of amino acid labeling of seeds imbibed with (^{15}N) ammonium for 24 h revealed that *asn3-1* seeds contained 20% less total asparagine while ^{15}N-labeled asparagine ((2-^{15}N)asparagine, (4-^{15}N)asparagine and (2,4-^{15}N)asparagine) increased by 12% compared to wild-type seeds. The data indicate a fine regulation of asparagine synthesis and hydrolysis in *Arabidopsis* seeds.

Keywords: amino acids; Arabidopsis thaliana; asparagine synthetase; nitrogen metabolism; seed nitrogen

1. Introduction

Higher plants take up inorganic nitrogen by absorbing nitrate and ammonium from the soil. Nitrate is reduced to ammonium by the combined action of nitrate reductase (NAD(P)H-NR, EC 1.7.1.1; EC 1.7.1.2; EC 1.7.1.3) and ferredoxin (Fd)-nitrite reductase (Fd-NiR, EC 1.7.1.4) while ammonium is also produced by photorespiration and the breakdown of nitrogenous compounds. It is then assimilated into glutamine and glutamate by glutamine synthetase (GS, EC 6.3.1.3) and glutamate synthase (GOGAT, EC 1.4.7.1 and EC 1.4.1.14) [1]. Asparagine synthetase (AS, EC 6.3.5.4) transfers the amide group of glutamine to aspartate, forming asparagine and glutamate. Asparagine, glutamine, aspartate and glutamate are important nitrogen carriers transported in the phloem; however, asparagine is a major nitrogen transporter since it contains more nitrogen per carbon (2N:4C) compared to glutamine (2N:5C), aspartate (1N:4C) and glutamate (1N:5C) [2,3].

Asparagine synthetase in *Arabidopsis thaliana* is encoded by three genes: *ASN1* (At3g47340), *ASN2* (At5g65010) and *ASN3* (At5g10240) [4]. All plants appear to contain a small *ASN* gene family consisting of two or three members [3]. A phylogenetic analysis has grouped *ASN1* in dicot-subclass I while *ASN2* and *ASN3* were placed in dicot-subclass II [3]. Class I *ASN* genes are differentially regulated, when compared to class II *ASN*, by light, sugars and inorganic/organic nitrogen metabolites [5,6], thus suggesting a different physiological function. Several lines of evidence indicate that *ASN1*-encoded asparagine synthetase plays a role in nitrogen export from source to sink organs via the phloem in the dark [7] and in the recapture of ammonium produced under biotic and abiotic stresses in *Arabidopsis* [7]. Loss-of-function studies of *ASN2*-deficient mutants provided evidence that *ASN2*-encoded asparagine synthetase is involved in leaf primary nitrogen assimilation during the vegetative stage [8] and in ammonium detoxification under abiotic stress [9].

On the other hand, little is known about the physiological role of *ASN3*-encoded asparagine synthetase. The aim of this study was to examine the impact of *ASN3* disruption so as to decipher the role of *ASN3*-encoded asparagine synthetase during vegetative growth, seed development and germination using *Arabidopsis* T-DNA insertion mutants affected in *ASN3* expression.

2. Materials and Methods

2.1. Isolation of Homozygous ASN3 T-DNA Insertion Lines

Seeds of T-DNA mutagenized *Arabidopsis thaliana* (Col-0 ecotype) for *asn3-1* (SALK_053490) and *asn3-2* (SALK_074279) were obtained from the Nottingham Arabidopsis Stock Centre (Nottingham, UK). Homozygous mutants were PCR-screened with gene-specific primers and a T-DNA border primer. The first PCR was carried out using the following gene-specific primers: *ASN3-1*: left primer (LP): 5′-GGAATTTTCCGGAGACAAAAC-3′, right primer (RP): 5′-GCAGAGTGCTGCTAGAGCAAC-3′; *ASN3-2*: LP: 5′-TTGCATGAACCAACCTAAACC-3′, RP: 5′-AGAAATGGGTGTTACGCAATG-3′. The PCR program consisted of one cycle at 95 °C for 3 min, 35 cycles of 94 °C for 30 s, 58 °C for 1.5 min, 72 °C for 1.5 min and one cycle at 72 °C for 10 min. The second PCR analysis used a gene-specific primer and the LBb1 border primer: 5′-GCGTGGACCGCTTGCTGCAATT-3′. Amplified fragments were visualized by ethidium bromide in agarose gels.

2.2. Plant Growth

Arabidopsis thaliana wild-type and *asn3* mutants were grown in a growth chamber (16 h light at 21 °C with 150 μmol photons $m^{-2} \cdot s^{-1}$ and 8 h dark at 17 °C) using a standard nutrient solution with 10 mM NO_3^{-1} as nitrogen source [10]. The complete solution contained 1.1 mM KH_2PO_4, 0.8 mM $MgSO_4$, 3.9 mM KNO_3, 3.1 mM $Ca(NO_3)_2$, 0.2 mM NaCl, 23 μM H_3BO_3, 9.0 μM $MnSO_4$, 0.3 μM $(NH_4)_6Mo_7O_{24}$, 1.0 μM $CuSO_4$ and 3.5 μM $ZnSO_4$ and 10 mg·L^{-1} Fe-EDTA (Sequestrene). Rosette leaves and fourth siliques numbered from the top of 35-day-old plants were harvested 3 h into the light period and immediately frozen in liquid nitrogen prior to analysis.

2.3. Real-Time Quantitative RT-PCR Analysis

Leaf total RNA was extracted using the RNeasy kit (Qiagen, Courtaboeuf, France). For seeds, total RNA was isolated by vortexing seed powder with the following reagent (100 mM LiCl, 100 mM Tris, pH 8.0, 10 mM EDTA, 1% SDS and 1.5% β-mercaptoethanol) with acidic phenol, pH 4.0. After centrifugation, the supernatant was extracted by acidic phenol/chloroform 5:1 and centrifuged. An equal volume of 8 M LiCl was added to the supernatant, kept at −80 °C, and RNA was recovered by centrifugation at 14000× *g* for 15 min. After a DNase treatment, the synthesis of cDNA was carried out using 2 μg RNA and the Omniscript RT kit (Qiagen, Courtaboeuf, France). Quantitative real-time RT-PCR (qPCR) was carried out using Takyon™ RoxSYBR MasterMixdTT Blue according to the manufacturer's instructions (Eurogentec, Seraing, Belgium). Amplification was carried out in a total volume of 20 μL and the following program: 40 cycles of 95 °C for 5 s, 55 °C for

15 s and 68 °C for 40 s using a BIO-RAD CFX Connect Real-Time System (Bio-Rad Laboratories, Marnes-la-Coquette, France). For isogenes, primer sets were designed using gene specific DNA regions and the sequences were as follows [5' to 3']: *ACT2* (At3g18780): F: CTTGCACCAAGCAGCATGAA, and R: CCGATCCAGACACTGTACTTCCTT: *AGT1* (At2g13360) F: CACAACGAGACCGCGACCG and R: CACCGTCCACTAGCAGCAAAG; *ASN3* (At510240) F: GGTCCAAGTGTGGCATGTAGC and R: CAATGGCTGGAGTCTTCTCTGC; *ASPGA1* (At5g08100) F: TTGACTGAGGCAGCGGCTTA and R: TCGCTAGCACAAGCCCTGAA; *ASPGB1* (At3g16150) F: TGGTGTGTCGTGTACCGGAG and R: GCAATGAGTCCAGCGAACCC: *GLN1;2* (At1g66200) F: TCTCAGACAACAGTGAAAAGATCA and R: TGTCTTGACCAGGAGCTTGAC. Melting curves were monitored to confirm amplification specificity. The results are expressed relative to *Actin 2* (*ACT2*) as a reference gene.

2.4. In Situ *Hybridization*

Leaf fixation and 8-μm-section microtome preparations of *Arabidopsis* rosette leaves were carried out as described in [8]. Hybridization probes were prepared from cDNA strands synthesized from 2 μg total RNA using an Omniscript RT kit (Qiagen, GmbH, Germany). Sense and antisense DNA fragments were amplified by PCR using *ASN3*-specific primers and by introducing the T7 sequence (5'-TGTAATACGACTCACTATAGGGC-3') at the 5'-end of both reverse and forward primers: *ASN3* forward primer: 5'-TACCAGGAGGTCCAAGTGTGG-3' and *ASN3* reverse primer: 5'-CAATGGCTGGAGTCTTCTCTGC-3'. Amplified sense and antisense DNA fragments (400 ng each) were reverse-transcribed with a Promega transcription kit (Madison WI, USA) using digoxigenin (DIG)-UTP and subjected to DNase digestion. *In situ* hybridization was carried out as described in [8] except for (not include in the steps) the incubation of leaf sections with secondary anti-DIG antibody conjugated to alkaline phosphatase. The visualization of *ASN3* RNA by alkaline phosphatase activity was carried out with sealed slides and fluorescence observed using a Leica DMR microscope (Leica Microsystems, Wetzlar, Germany).

2.5. Western Blot Analysis

Total soluble proteins were extracted by grinding in an extraction buffer consisting of 50 mM sodium phosphate buffer, pH 7.5, 5 mM EDTA and 14 mM β-mercaptoethanol. After centrifugation at $14000\times g$ for 15 min, the supernatant was recovered. Denatured proteins were subjected to SDS-PAGE using 7% gels [11]. Proteins were transferred to a nitrocellulose membrane and probed with rabbit antibodies raised against *Arabidopsis* recombinant *ASN2*-encoded asparagine synthetase [8]. After hybridization with goat serum anti-rabbit antibodies conjugated with a peroxidase, ASN protein was detected by the peroxidase activity in the presence of 3.4 mM 4-chloro-1-naphtol and 0.01% (*v*/*v*) H_2O_2. Protein intensities were estimated using Multi Gauge V3.2 software (Fuji Film, Bois d'Arcy, France).

2.6. Chlorophylls and Ammonium Measurements

Total chlorophyll contents were measured by the method of Arnon [12]. Free ammonium contents were determined by a phenol hypochlorite assay [8].

2.7. Quantitative Amino Acid PROFILING

Total soluble metabolites were extracted and quantified by GC-MS according to Fiehn [13]. The GC-MS analysis was performed using an Agilent 7890A gas chromatograph coupled to an Agilent 5975C mass spectrometer as described in [8]. Peaks were identified using the AMDIS 32 software after retention index (RI) calibration with an alkane mix (C10, C12, C15, C19, C22, C28, C32, C36) injected during the course of the analysis. Statistical analyses by permutation (Student's *t*-test and 1 Way-ANOVA) were performed using the MeV software [14].

2.8. ^{15}N Labeling Analysis

The ^{15}N labeling analysis was carried out on three sets each comprising more than 150 seeds using the same initial weight per genotype. Seeds were incubated with 2 mM [^{15}N]ammonium (99% enrichment) (Euriso-top S.A., Saint-Aubin, France) in Petri dishes at 20 °C in darkness and harvested after 24 h. Amino acids were extracted with 50% methanol (*v/v*) containing 100 μM methionine sulfone as an internal control to normalize amino acid contents. After centrifugation, the supernatant was filtered and analyzed by a capillary electrophoresis system coupled to a mass spectrophotometer (CE/MS) according to Takahashi *et al.* [15]. For capillary electrophoresis, a fused silica capillary (0.050 mm internal diameter; GL Sciences, Torrance, CA, USA) was used with a 1 M formic acid (pH 1.5) elution solution at +24 V and at 20 °C. The sheath solution was a mixture of 0.1% (*w/v*) formic acid and 50% (*v/v*) methanol with positive-mode detection.

3. Results

3.1. Characterization of asn3 Mutants

The *Arabidopsis* genome database [4] contains three functional genes for asparagine synthetase (AS): *ASN1* (At3g47340), *ASN2* (At5g65010) and *ASN3* (At5g10240). *Arabidopsis* T-DNA insertion lines for the *ASN3* gene were PCR-screened and mutants containing a T-DNA insertion either in intron 13 or in exon 14 were isolated. Homozygous lines were PCR-selected and named *asn3-1* (SALK_053490) and *asn3-2* (SALK_074279), respectively (Figure 1a).
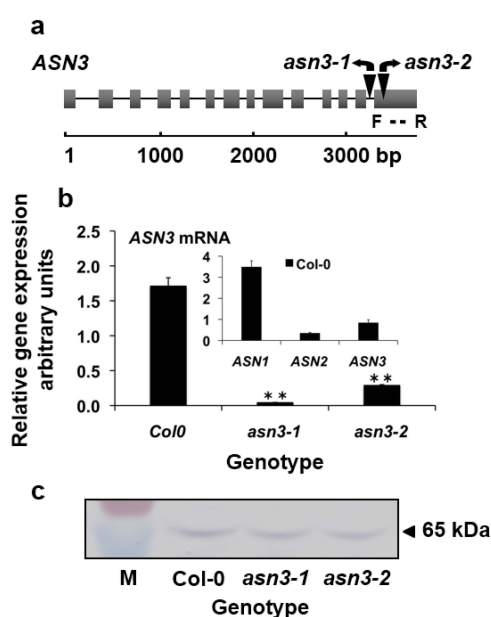

Figure 1. Characterization of *asn3-1* and *asn3-2* T-DNA insertion mutants using rosette leaves from 35-day-old Arabidopsis plants. (**a**) Schematic presentation of the T-DNA insertion site within the *ASN3* gene of the *asn3-1* (intron 13) and *asn3-2* (exon 14) lines; (**b**) *ASN1* mRNA, *ASN2* mRNA and *ASN3* mRNA levels of wild-type (Col-0) (insert), and *ASN3*mRNA levels in wild-type (Col-0), *asn3-1* and *asn3-2* lines; (**c**) Western blot showing asparagine synthetase protein in wild-type (Col-0), *asn3-1* and *asn3-2* lines. Boxes and lines in the gene structure correspond to exons and introns, respectively. Black triangles indication T-DNA insertions (the size is not to scale). *ASN3* mRNA levels were measured by qPCR relative to *Actin 2* (At3g18780) and expressed as the mean ± SE of three biological replicates. F and R represent forward and reverse primers, respectively. Asterisks indicate significant differences between the Col-0 and *asn3* mutants using a Student's *t*-test *P*-values ** $p < 0.01$. Molecular mass markers on the Western blot membrane (M) correspond to 55 kDa and 72 kDa (Thermo Fisher Scientific Inc, Villebon-sur-Yvette, France).

The phenotypic analysis was carried out using rosette leaves from 35-day-old plants. A qPCR analysis showed that wild-type leaves contained *ASN3* mRNA levels that were lower than *ASN1* but higher than *ASN2* (Figure 1b). The *asn3-1* and *asn3-2* lines contained 2.4% and 17% of wild-type RNA levels, respectively (Figure 1b). Asparagine synthetase protein abundance in total soluble proteins of green leaves was examined by Western blots probed with antibodies raised against *Arabidopsis* recombinant *ASN2*-encoded asparagine synthetase [8]. It was assumed that the observed 65 kDa band on the membrane contained the three asparagine synthetase isoforms encoded by *ASN1*, *ASN2* and *ASN3* with molecular masses of 65.5 kDa, 65 kDa and 65.2 kDa, respectively, and that the asparagine synthetase 2 antibody cross-reacted with epitopes of asparagine synthetase 3 since the three asparagine synthetases share a 87% to 92% amino acid similarity [3]. This indicated that rosette leaves of *asn3-1* and *asn3-2* lines displayed asparagine synthetase protein contents that were similar to wild-type (WT) plants (Figure 1c).

3.2. Cellular Expression of ASN3 mRNA and Phenotypic Analysis of asn3 Mutants

As our aim was to evaluate the function of *ASN3*-encoded asparagine synthetase in *Arabidopsis* development, comparative phenotypic analyses were carried out on both *asn3* mutants and Col-0 plants. Because the function of asparagine synthetase is closely related to cellular localization, cell-specific expression patterns of *ASN3* mRNA were first determined by *in situ* hybridization. Thin leaf sections were hybridized with either antisense or control sense *ASN3* probes. A specific brown signal was associated with the companion cell/sieve tube element complex within the minor veins (Figure 2a).
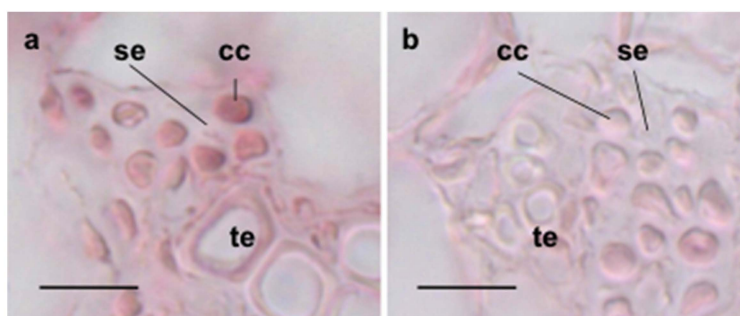

Figure 2. *In situ* hybridization of *ASN3* mRNA in *Arabidopsis* leaves with (**a**) antisense *ASN3* mRNA and (**b**) control sense *ASN3* mRNA. Digoxigenin (DIG)-UTP-labeled *in situ* hybridization signals were detected by microscopy. cc: companion cell, se: sieve element, te: tracheary element. Bar = 20 μm.

The specificity of the signal was controlled by hybridization of leaf sections with a sense *ASN1* mRNA probe which gave no specific signal (Figure 2b).

A phenotypic analysis of the *asn3-1* and *asn3-2* lines was carried out 35 days after sowing at the vegetative stage and compared with the Col-0 line. No visible phenotype was detected for the *asn3-1* and *asn3-2* mutants (Figure 3a). Both *asn3-1* and *asn3-2* rosette leaves contained wild-type levels of chlorophyll (Figure 3b) and ammonium content (Figure 3c), indicating that *ASN3* disruption did not cause a defective nitrogen status during vegetative growth. During seed development, leaves and stems serve as source tissues to supply nitrogen resources to developing siliques which in turn deliver nitrogen to seeds. As asparagine is one of the primary nitrogen carriers from the source to sink organs, the impact of *ASN3* disruption on asparagine, glutamine, aspartate and glutamate levels was investigated in *asn3-1* siliques and compared to the WT situation. Fourth siliques numbered from the top of the plants at stage 8 [16], mainly containing early- to late-heart-stage embryos, were harvested. Soluble metabolites were quantified by GC-MS, and differences were expressed as $\log_2([\text{amino acid}]_{asn3-1}/[\text{amino acid}]_{Col-0})$. The young siliques of the *asn3-1* knockout line showed an increase in glutamine (Gln_{asn3-1} to Gln_{Col-0} ratio of 1.014), glutamate (Glu_{asn3-1} to Glu_{Col-0} ratio of 1.189) and aspartate (Asp_{asn3-1} to Asp_{Col-0} ratio of 1.149) and a decrease in asparagine (Asn_{asn3-1} to

Asn_{Col-0} ratio of 0.902) (Figure 3d). To evaluate the effect of *ASN3* disruption on nitrogen remobilization to seeds (the ultimate sink organ), the total nitrogen and carbon contents of dry seeds were determined using a micro-Carbon Nitrogen (CN) analyzer. The total nitrogen and total carbon contents of *asn3-1* and *asn3-2* seeds were not statistically different from those of the wild type (Figure 3e).
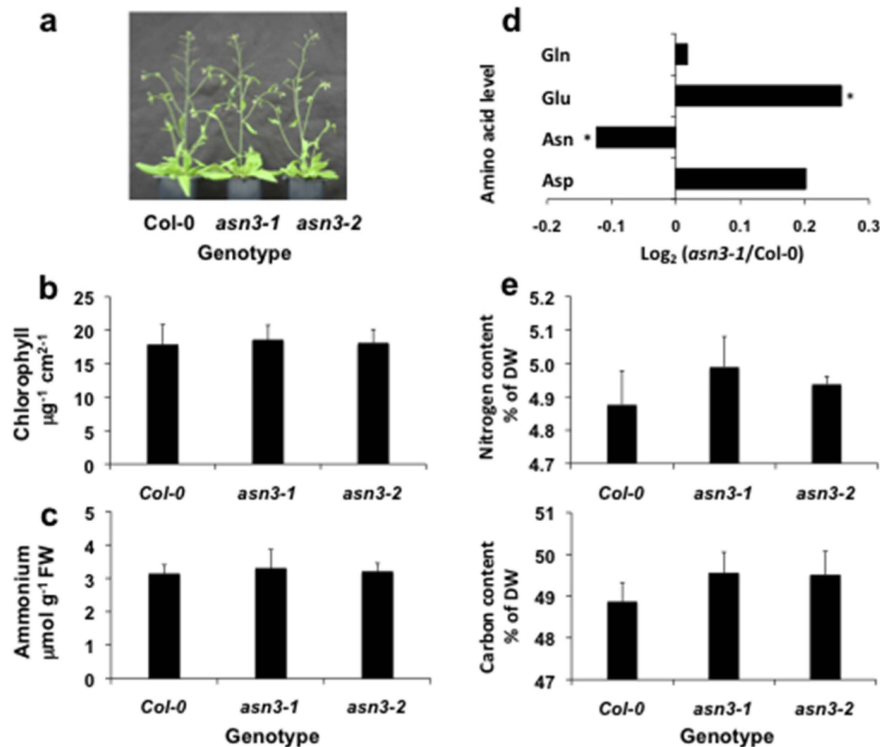

Figure 3. Phenotypic analysis of *Arabidopsis asn3-1* and *asn3-2* lines. (**a**) Representative visual growth phenotype; (**b**) chlorophyll content; and (**c**) ammonium content in rosette leaves of 35-day-old wild-type (Col-0), *asn3-1* and *asn3-2* rosettes; (**d**) ratios of selected amino acid contents in young siliques of Col-0 and *asn3-1* expressed as Log_2 [amino acid]$_{asn3-1}$/[amino acid]$_{Col-0}$. A positive value represents a higher metabolite content in the *asn3-1* line, and a negative value corresponds to a lower metabolite content in the *asn3-1* line; (**e**) total nitrogen and carbon contents in dry seeds of Col-0, *asn3-1* and *asn3-2* lines. The values represent the mean ± SE of three biological replicates. Asterisks indicate significant differences between the wild-type and transgenic lines with a Student's *t*-test *p* values * $p < 0.05$.

3.3. ^{15}N Labeling of Amino Acids in Germinating asn3 Seeds

Seed imbibition triggers quiescent seeds to become highly metabolic embryonic cells [17] in which nitrogen mobilization takes place for the synthesis of amino acids required for developing embryonic organs. Asparagine is one of the major free amino acids in the germinating seeds of *Arabidopsis*, serving to translocate nitrogen within the seed. To investigate the physiological function of *ASN3*-encoded asparagine synthetase in germinating seeds, expression profiles of genes involved in asparagine metabolism including *ASN3*, *GLN1;2* (At1g66200), *ASPGA1* (At5g08100), *ASPGB1* (At3g16150) and *AGT1* (At2g13360) were determined in 24 h–imbibed seeds.

Figure 4 shows the pathways of asparagine metabolism. *GLN1;2* codes for a cytosolic GS1 that supplies glutamine for glutamine synthetase activity. *ASPGA1* and *ASPGB1* code for cytosolic asparaginase isoforms (ASPG, EC 3.5.1.1) and *AGT1* codes for peroxisomal asparagine aminotransferase (AsnAT, EC 2.6.1.45). Asparaginase and asparagine aminotransferase release the amide group and amino group of asparagine as ammonia, respectively, and both nitrogen groups are used for subsequent amino acid synthesis [18]. Total RNA was isolated from Col-0 and *asn3-1* seeds imbibed for 24 h, and

mRNA levels were measured by qPCR. The level of *ASN3* mRNA was reduced to 2.5% and 15% of the wild-type value in the seeds of *asn3-1* and *asn3-2*, respectively (Figure 5a).
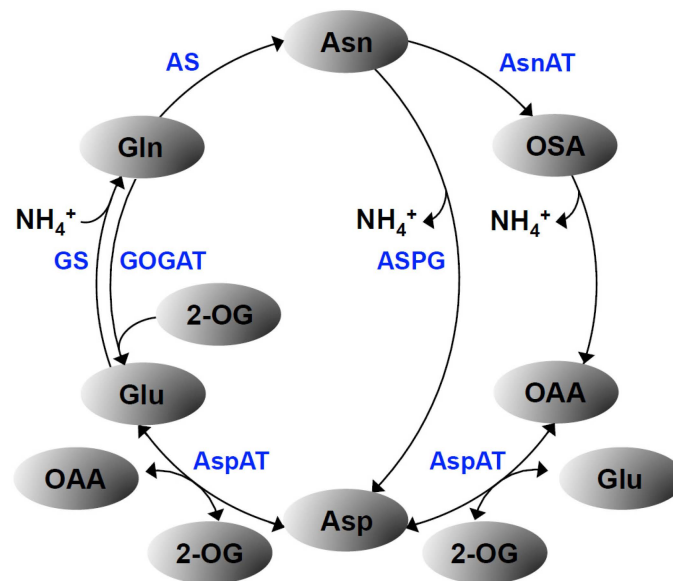
Figure 4. Schematic presentation of asparagine metabolism. AS: asparagine synthetase (EC 6.3.5.4), Asn: asparagine, AsnAT: asparagine aminotransferase (EC 2.6.1.45), Asp: aspartate, AspAT: aspartate aminotransferase (EC 2.6.1.1), ASPG: asparaginase (EC 3.5.1.1), Gln: glutamine, Glu: glutamate, GOGAT: glutamate synthase (Ferredoxin-GOGAT, EC 1.4.7.1 and NADH-GOGAT, EC 1.4.1.14), GS: glutamine synthetase (EC 6.3.1.2), OAA: oxaloacetate, 2-OG: 2-oxoglutarate, OSA: 2-oxosuccinamate.

Similar *GLN1;2* and *AGT1* mRNA levels were detected in wild-type and *asn3* seeds. Of the two *ASPG* genes, *ASPGB1* showed higher mRNA levels than *ASPGA1* in both wild-type and *asn3* seeds (Figure 5a).

To investigate the function of *ASN3*-encoded asparagine synthetase in the synthesis of amino acids in seeds, ^{15}N labeling patterns of glutamine, glutamate, asparagine and aspartate were accessed by focusing on the *asn3-1* knockout line. Wild-type Col-0 and *asn3-1* seeds were incubated with ^{15}[N]ammonium (99% enrichment) for 24 h in the dark at 20 °C, and the total amino acids were extracted. The labeling of glutamine, glutamate, asparagine and aspartate was analyzed using a capillary electrophoresis system coupled to a mass spectrophotometer as described in the Materials and Methods (2.8). When compared to wild-type seeds, *asn3-1* seeds displayed reduced glutamine (by 30%), asparagine (20%) and aspartate (20%) contents while exhibiting increased glutamate (10%) amounts (Figure 5b; Table S1). When control Col-0 seeds were incubated with [^{15}N]ammonium for 24 h, ^{15}N-labeled glutamine ([5-^{15}N]glutamine + [2-^{15}N]glutamine and [2,5-^{15}N]glutamine) accounted for 79% of the total glutamine (Figure 5b; Table S1). A lower percentage of labeling was detected for glutamate ([2-^{15}N]glutamate) (26%), aspartate ([2-^{15}N]aspartate) (32%) and asparagine ([2-^{15}N]asparagine + [4-^{15}N]asparagine and [2,4-^{15}N]asparagine) (30%) (Figure 5b; Table S1), thus indicating an active GS in wild-type seeds. Interestingly, *asn3-1* seeds showed a lower percentage of ^{15}N-labeled glutamine than Col-0 seeds (66% *versus* 79%) (Figure 5b; Table S1) while they contained enhanced ^{15}N-labeled asparagine (42% *versus* 30%) and glutamate (28% *versus* 26%) when compared to Col-0 seeds (Figure 5b; Table S1). Aspartate was equally labeled in both wild-type and *asn3-1* lines (Figure 5b; Table S1).
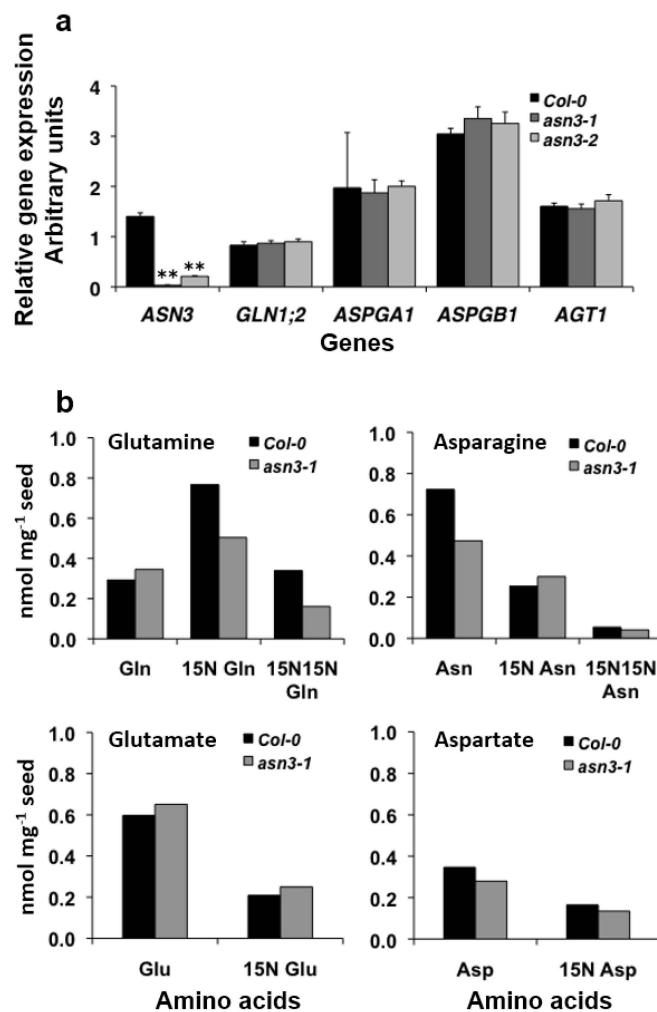
Figure 5. Comparison of (**a**) mRNA levels of *ASN3*, *GLN1;2*, *ASPGA1*, *ASPGB1* and *AGT1* and (**b**) ^{15}N labeling of glutamine, glutamate, asparagine and aspartate in Col-0 and *asn3-1* seeds imbibed for 24 h. A qRT-PCR analysis was carried out to estimate mRNA levels of *ASN3* (At5g10240) coding for asparagine synthetase, *GLN1;2* (At1g66200) for cytosolic GS1, *ASPGA1* (At5g08100) and *ASPGB1* (At3g16150) for asparaginase and *AGT1* (At2g13360) for asparagine aminotransferase. Transcript levels, relative to *Actin* 2 (At3g18780) as a reference gene, are expressed as the mean $\pm$ SE of three biological replicates. The ^{15}N labeling analysis was carried out on three sets, each comprising more than 150 seeds using the same initial weight per genotype to determine single labeling (^{15}N glutamine, ^{15}N glutamate, ^{15}N asparagine, ^{15}N aspartate) and double labeling (^{15}N^{15}N glutamine, ^{15}N^{15}N asparagine). Asterisks indicate significant differences between wild-type and transgenic lines with Student's *t* test *p*-values ** $p < 0.01$.

4. Discussion

Three *ASN* genes encode asparagine synthetase in *Arabidopsis*, and little is known about the role of asparagine synthetase encoded by *ASN3*. We assessed the physiological role of *ASN3*-encoded asparagine synthetase in nitrogen metabolism at three developmental stages including vegetative growth, seed maturation and seed germination. During vegetative growth, *asn3-1* knockout and *asn3-2* knockdown mutant leaves displayed wild-type asparagine synthetase protein, chlorophylls and ammonium contents and no visible phenotype (Figure 3). A weak effect of *ASN3* disruption at this stage of development can be associated with lower *ASN3* expression levels relative to *ASN1* and *ASN2* in vegetative leaves, as indicated by qPCR (Figure 1; [8]). Also, lower *ASN3* mRNA levels

have been reported by transcriptomics analysis of eight-day-old whole seedlings (expression ratio of *ASN1:ASN2:ASN3* = 1.7:5.5:1), young rosette leaf *n* = 6 (*ASN1:ASN2:ASN3* = 0.4:7:1) and seeds at the green cotyledon stage (*ASN1:ASN2:ASN3* = 22:0.1:1) [19]. However, among seven organs under different developmental stages, higher *ASN3* mRNA levels were reported for the seven-day-old shoot apex (*ASN1:ASN2:ASN3* = 0.2:0.6:1) [19]. Despite the low mRNA level measured by qPCR, our *in situ* mRNA hybridization analysis localized *ASN3* mRNA to companion cells that are in close vicinity to the sieve element of the leaf phloem vasculature (Figure 2), allowing a symplastic loading of asparagine into the phloem sieve element for export. As amino acids and peptides serve to translocate nitrogen through the phloem from source to sink organs, it was interesting to find that the asparagine content of *asn3-1* siliques was reduced while the glutamate content was enhanced (Figure 3d). However, although siliques remobilize nitrogen to developing seeds during embryogenesis and maturation [7], the total nitrogen contents of dry seeds of Col-0, *asn3-1* and *asn3-2* were found to be similar (Figure 3), suggesting that *ASN3* disruption did not affect seed nitrogen status.

During nitrogen mobilization in seeds imbibed for 24 h, exogenous (^{15}N)ammonium was assimilated into amino acids in both the Col-0 and *asn3-1* lines (Figure 5; Table S1). The *asn3-1* seeds exhibited changes in amino acid composition and (^{15}N)amide and (^{15}N)amino acid labeling patterns. In particular, a 20% reduction of the total asparagine content in the *asn3-1* seeds relative to the Col-0 seeds could be caused by a reduced supply of non-labeled amino acids from the seed (0.47 nmol· mg^{-1} seed in *asn3-1* and 0.72 nmol· mg^{-1} seed in Col-0) due to the disruption of *ASN3*, while ^{15}N-labeled asparagine ((2-^{15}N)asparagine + (4-^{15}N)asparagine and (2,4-^{15}N)asparagine) was enhanced from 30% in Col-0 seeds to 42% in *asn3-1* seeds (Figure 5; Table S1). The increase in the amount of labeled asparagine in germinated *asn3-1* seeds, depending on its synthesis and hydrolysis, could be associated with a low availability of labeled aspartate and glutamine, precursors for asparagine synthesis. This is in agreement with the lower aspartate content and contrasting higher glutamate level in *asn3-1* seeds compared to Col-0 seeds despite the reversible transamination reaction between aspartate and glutamate catalyzed by aspartate aminotransferase (EC 2.6.1.1) (Figure 5; Table S1). The *asn3-1* seeds displayed a lower total content of ^{15}N-labeled amino acids (glutamine, glutamate, asparagine and aspartate) than Col-0 seeds. This decline in *asn3-1* seeds was associated with lower amounts of ^{15}N-labeled glutamine and aspartate and with higher ^{15}N-labeled asparagine and glutamate levels (Figure 5b; Table S1). These altered ^{15}N labeling patterns of glutamine, asparagine, glutamate and aspartate might be correlated with a lower GS activity and increased asparagine synthetase and glutamate synthase activities in *asn3-1* seeds. Since *GLN1;2* expression was similar in *asn3* and wild-type seeds, the reduced glutamine content could reflect an altered utilization rather than a modified synthesis. Likewise, the lower content of non-labeled asparagine could be associated with its hydrolysis by asparaginase into ammonium and aspartate, which is reversibly transaminated to glutamate, and asparagine aminotransferase that produces 2-oxosuccinamate which is converted to ammonium and oxaloacetate by ω-amidase (EC 3.5.1.3) [20]. This would produce intermediates to feed the tricarboxylic acid (TCA) cycle (oxaloacetate, 2-oxoglutarate, and malate) and the γ-aminobutyric acid (GABA) shunt (glutamate) for amino acid synthesis and energy generation at the expense of asparagine. It was found that germinating *asn3-1* seeds expressed wild-type *ASPGA1* and *ASPGB1* mRNA levels (Figure 5). However, a promoter analysis of *ASPGA1::GUS* demonstrated an expression in seed epidermal cells that began 24 h after sowing [21], suggesting an implication of asparaginase in asparagine hydrolysis. Moreover, the imbibed *asn3-1* seeds contained wild-type levels of *AGT1* mRNA (Figure 5). *AGT1* is the single gene encoding serine:glyoxylate aminotransferase which catalyzes transamination reactions with multiple substrates including asparagine as an amino donor [22–24]. Previous studies demonstrated that *Arabidopsis* asparagine aminotransferase acts as a serine:glyoxylate aminotransferase [24]. During photorespiration in leaves, this peroxisomal aminotransferase catalyzes the transamination of serine with glyoxylate to give glycine and hydroxypyruvate. Thus, asparagine aminotransferase might play a role in detoxifying glyoxylate which can inhibit RuBisCO activity. Both the wild-type expression level of *AGT1* and its high catalytic efficiency, expressed as V_{max}/K_m, of

asparagine aminotransferase (10.4×10^{-8} kcat mg$^{-1} \cdot$ mM^{-1}), are similar to that of *ASPGB1*-encoded asparaginase (9.72×10^{-8} kcat mg$^{-1} \cdot$ mM^{-1}) [24,25], thus suggesting that asparagine hydrolysis not only provides ammonium but also pre-conditions aspartate and glutamate in response to the lower energy status of the germinating seeds. Despite *ASN3* disruption, increased levels of ^{15}N-labeled asparagine in *asn3-1* seeds may be due to the decreased endogenous asparagine content, suggesting that *ASN3*-encoded asparagine synthetase may contribute to providing at least a basal level of asparagine in germinating seeds. Indeed, our data are in agreement with a fine regulation of substrate supply to asparagine synthesis and its hydrolysis in *Arabidopsis* organs.

References

1. Coruzzi, G.M. Primary N-assimilation into amino acids in *Arabidopsis*. In *The Arabidopsis Book*; Somerville, C., Meyerrowitz, E., Eds.; American Society of Plant Biologists: Rockville, MD, USA, 2003; pp. 1–17.

2. Lea, P.J.; Sodeck, L.; Parry, M.A.J.; Shewry, P.R.; Halford, N.G. Asparagine in plants. *Ann. Appl. Biol.* **2007**, *150*, 1–26. [CrossRef]

3. Gaufichon, L.; Reisdorf-Cren, M.; Rothstein, S.J.; Chardon, F.; Suzuki, A. Biological functions of asparagine synthetase in plants. *Plant Sci.* **2010**, *179*, 141–153. [CrossRef]

4. Arabidopsis Genome Initiative. Analysis of the genome sequence of the flowering plant *Arabidopsis thaliana*. *Nature* **2000**, *408*, 796–815.

5. Herrera-Rodriguez, M.B.; Maldonado, J.M.; Perez-Vicente, R. Light and metabolic regulation of *HAS1, HAS1.1* and *HAS2*, three asparagine synthetase genes in *Helianthus annuus*. *Plant Physiol. Biochem.* **2004**, *42*, 511–518. [CrossRef] [PubMed]

6. Bläsing, O.E.; Gibon, Y.; Günther, M.; Höhne, M.; Morcuende, R.; Osuna, D.; Thimm, O.; Björn, U.; Scheobe, W.-R.; Stitt, M. Sugars and circadian regulation make major contributions to the global regulation of diurnal gene expression in *Arabidopsis*. *Plant Cell* **2005**, *17*, 3257–3281. [CrossRef] [PubMed]

7. Lam, H.-M.; Wong, P.; Chan, H.-K.; Yam, K.-M.; Cheng, L.; Chow, C.-M.; Coruzzi, G.M. Overexpression of the *ASN1* gene enhances nitrogen status in seeds of Arabidopsis. *Plant Physiol.* **2003**, *132*, 926–935. [CrossRef] [PubMed]

8. Gaufichon, L.; Masclaux-Daubresse, C.; Tcherkez, G.; Reisedorf-Cren, M.; Sakakibara, Y.; Hase, T.; Clément, G.; Avice, J.-C.; Grandjean, O.; Marmagne, A.; *et al.* *Arabidopsis thaliana ASN2* encoding asparagine synthetase is involved in the control of nitrogen assimilation and export during vegetative growth. *Plant Cell Environ.* **2013**, *36*, 328–342. [CrossRef] [PubMed]

9. Wong, H.-K.; Chan, H.-K.; Coruzzi, G.M.; Lam, H.-M. Correlation of *ASN2* gene expression with ammonium metabolisms in Arabidopsis. *Plant Physiol.* **2004**, *134*, 332–338. [CrossRef] [PubMed]

10. Coïc, Y.; Lessaint, C. Comment assurer une bonne nutrition en eau et en ions minéreaux en holticulture? *Holticulture Fr.* **1971**, *8*, 11–14.

11. Laemmli, U.K. Cleavage of structural proteins during the assembly of bacteriophage T4. *Nature* **1970**, *227*, 680–685. [CrossRef] [PubMed]

12. Arnon, D.I. Copper enzymes in isolated chloroplasts. Polyphenol oxidase in *Beta vulgaris* L. *Plant Physiol.* **1949**, *24*, 1–15. [CrossRef] [PubMed]

13. Fiehn, O. Metabolic profiling in *Arabidopsis*. *Method Mol. Biol.* **2006**, *323*, 439–447.

14. Saeed, A.I.; Sharov, V.; White, J.; Li, J.; Liang, W.; Bhagabati, N.; Braisted, J.; Klapa, M.; Currier, T.; Thiagarajan, M.; *et al.* TM4: A free, open-source system from microarray data management and analysis. *Biotechniques* **2003**, *34*, 374–378. [PubMed]

15. Boyes, D.C.; Zayed, A.M.; Ascenzi, R.; McCaskill, A.J.; Hoffman, N.E.; Davis, K.R. Growth stage-based phenotypic analysis of Arabidopsis: A model for high throughput functional genomics in plants. *Plant Cell* **2001**, *13*, 1499–1510. [CrossRef] [PubMed]

16. Takahashi, H.; Hayashi, M.; Goto, F.; Sato, S.; Soga, T.; Nishioka, T.; Tomita, M.; Kawai-Yamada, M.; Uchimiya, H. Evaluation of metabolic alteration in transgenic rice overexpressing dihydroflavonol-4-reductase. *Ann. Bot.* **2006**, *98*, 819–825. [CrossRef] [PubMed]

17. Gallardo, K.; Job, C.; Groot, S.P.C.; Puype, M.; Demol, H.; Vandekerckhove, J.; Job, D. Proteomics of Arabidopsis seed germination. A comparative study of wild-type and gibberellin-deficient seeds. *Plant Physiol.* **2007**, *129*, 823–837. [CrossRef] [PubMed]

18. Ireland, R.J.; Lea, P.J. The enzymes of glutamine, glutamate, asparagine and aspartate metabolism. In *Plant Amino Acids*; Singh, B.K., Ed.; Marcel Dekker, Inc.: New York, NY, USA; Basel, Switzerland; Hong Kong, China, 1999; pp. 49–109.

19. Schmid, M.; Davidson, T.S.; Hnz, S.; Pap, U.J.; Demar, M.; Vingron, M.; Schölkopf, B.; Weigel, D.; Lohmann, J.U. A gene expression map of *Arabidopsis thaliana* development. *Nat. Genet.* **2005**, *37*, 501–506. [CrossRef] [PubMed]

20. Zhang, Q.; Marsolais, F. Identification and characterization of omega-amidase as an enzyme metabolically linked to asparagine transamination in Arabidopsis. *Phytochemisty* **2014**, *99*, 36–43. [CrossRef] [PubMed]

21. Ivanov, A.; Kameka, A.; Pajak, A.; Bruneau, L.; Beyaert, R.; Hernández-Sebastià, C.; Marsolais, F. *Arabidopsis* mutants lacking asparaginases develop normally but exhibit enhanced root inhibition by exogenous asparagine. *Amino Acids* **2012**, *42*, 2307–2318. [CrossRef] [PubMed]

22. Joy, K.W.; Prabha, C. The role of transamination in the synthesis of homoserine in peas. *Plant Physiol.* **1986**, *82*, 99–102. [CrossRef] [PubMed]

23. Liepman, A.H.; Olsen, L.J. Peroxisomal alanine:glyoxylate aminotransferase (AGT1) is a photorespiratory enzyme with multiple substrates in *Arabidopsis thaliana*. *Plant J.* **2001**, *25*, 487–498. [CrossRef] [PubMed]

24. Zhang, Q.; Lee, J.; Pandurangan, S.; Clark, M.; Pajak, A.; Marsolas, F. Characterization of Arabidopsis serine: Glyoxylate aminotransferase, AGT1, as an asparagine aminotransferase. *Phytochemistry* **2013**, *85*, 30–35. [CrossRef] [PubMed]

25. Gabriel, M.; Telmer, P.G.; Marsolais, F. Role of asparaginase variable loop at the carboxyl terminal of the alpha subunit in the determination of substrate preference in plants. *Planta* **2012**, *235*, 1013–1022. [CrossRef] [PubMed]